nature immunology

T cell receptor recognition of a 'super-bulged' major histocompatibility complex class I–bound peptide

Fleur E Tynan[1,5], Scott R Burrows[2,5], Ashley M Buckle[1,5], Craig S Clements[1], Natalie A Borg[1], John J Miles[2], Travis Beddoe[1], James C Whisstock[1], Matthew C Wilce[1], Sharon L Silins[2], Jacqueline M Burrows[2], Lars Kjer-Nielsen[3], Lyudmila Kostenko[3], Anthony W Purcell[4], James McCluskey[3] & Jamie Rossjohn[1]

Unusually long major histocompatibility complex (MHC) class I–restricted epitopes are important in immunity, but their 'bulged' conformation represents a potential obstacle to αβ T cell receptor (TCR)–MHC class I docking. To elucidate how such recognition is achieved while still preserving MHC restriction, we have determined here the structure of a TCR in complex with HLA-B*3508 presenting a peptide 13 amino acids in length. This complex was atypical of TCR–peptide–MHC class I interactions, being dominated at the interface by peptide-mediated interactions. The TCR assumed two distinct orientations, swiveling on top of the centrally bulged, rigid peptide such that only limited contacts were made with MHC class I. Although the TCR-peptide recognition resembled an antibody-antigen interaction, the TCR–MHC class I contacts defined a minimal 'generic footprint' of MHC-restriction. Thus our findings simultaneously demonstrate the considerable adaptability of the TCR and the 'shape' of MHC restriction.

CD8$^+$ cytotoxic T lymphocytes (CTLs) generally recognize short peptide fragments[1] approximately nine amino acids in length, bound to major histocompatibility complex (MHC) class I molecules (pMHC-I)[2]. This recognition is genetically restricted to the MHC molecules of the host[3]. However, the underlying structural basis of this MHC restriction is unknown[4]. Nonetheless, the nature of T cell receptor (TCR) interactions with such pMHC-I complexes has been elucidated by many structural and biochemical studies[5,6] that have led to some general observations regarding this engagement. The TCR usually engages the pMHC-I in an approximately diagonal orientation, whereas MHC class II–restricted TCRs were initially considered to dock orthogonally[7]. However, considerable variations to such generalizations have been noted[8–10]. Typically up to three upward-facing, solvent-exposed residues from the antigenic peptide contribute directly to the TCR interaction[5]. Accordingly, relative to the bound peptide, the polymorphic MHC class I heavy chain dominates the interface, thereby defining the complexities underlying MHC restriction.

The size limitation of peptides binding to MHC class I is dictated in part by a highly conserved hydrogen-bonding network at the amino- and carboxy-terminal ends of the antigen-binding cleft[11–13]. However, the antigen-processing machinery also influences the length of MHC class I peptides through the concerted actions of the proteasome[14], the transporter associated with antigen processing[15,16] and aminopeptidase-trimming enzymes in the endoplasmic reticulum[16–18]. Despite these restrictions, some longer peptides can bind to MHC class I (refs. 19–26), where they generally bulge centrally from the antigen-binding cleft or occasionally can extend beyond the conventional carboxy-terminal anchor site[27]. Longer MHC class II peptides have even been noted to form hairpin turns at one terminus[28]. Some of these unusually long, bulging MHC class I peptides demonstrate substantial mobility[24] and might be easily displaced upon TCR ligation. In contrast, other longer peptides assume a more rigid conformation that has the potential to pose considerable steric obstacles to TCR ligation[26].

There is a growing appreciation of the role of longer peptides in MHC class I–restricted immunity, including evidence that these determinants can form natural targets for MHC-restricted CTLs in virus infections[25,26] and antitumor responses[24,29]. However, the strategy used by TCRs in recognizing bulged pMHC complexes is poorly understood. For example, it is not known whether the interaction of these TCRs is mainly peptide driven or whether they effectively deform the bulged peptide to facilitate docking. Nor is it known whether diagonal docking prevails or how MHC restriction is maintained in the recognition of such ligands.

In addressing these issues, the CTL response to a 13–amino acid peptide, LPEPLPQGQLTAY (LPEP), has been studied. LPEP is derived from positions 52–64 of the BZLF1 (ZEBRA) antigen of Epstein-Barr virus. This 13-residue Epstein-Barr virus determinant is presented by HLA-B*3508 (ref. 25), whereas the closely related HLA-B*3501 allotype induces CTL responses only to the overlapping 11-residue

[1]The Protein Crystallography Unit, Department of Biochemistry and Molecular Biology, School of Biomedical Sciences, Monash University, Clayton, Victoria 3800, Australia. [2]Cellular Immunology Laboratory, Queensland Institute of Medical Research, Brisbane 4029, Australia. [3]Department of Microbiology and Immunology and [4]Department of Biochemistry, University of Melbourne, Parkville, Victoria 3010, Australia. [5]These authors contributed equally to this work. Correspondence should be addressed to J.R. (jamie.rossjohn@med.monash.edu.au) or J.M. (jamesm1@unimelb.edu.au).

Received 12 June; accepted 23 August; published online 25 September 2005; doi:10.1038/ni1257

epitope EPLPQGQLTAY (positions 54–64). A single-residue polymorphism distinguishes HLA-B*3508 (Arg156) from HLA-B*3501 (Leu156) and controls differential peptide selection, even though HLA-B*3501 can bind the LPEP epitope *in vitro*[26]. The structures of both the HLA-B*3508–LPEP and HLA-B*3501–LPEP complexes have shown the peptide to be centrally bulged and rigid[26], indicating the peptide presents an obstacle to TCR ligation. Nonetheless, people with HLA-B*3508 generate a robust CTL response to LPEP that is notably biased in variable α-region (V_α region) usage and, to a lesser extent, V_β usage[26]. We reasoned that the steric obstacle presented by rigid, bulged peptides might constrain TCR–MHC class I contacts and give a clearer picture of the essential requirements for MHC restriction, thus providing a general mechanism for this central but unresolved hallmark of T cell immunity[4].

Here we describe the structure of a canonical TCR from a CTL clone, SB27, in complex with its cognate HLA-B*3508–LPEP ligand. We demonstrate that αβ TCR recognition of this unusually long epitope involved an orthogonal docking mode of TCR-pMHC binding that was dominated by peptide-mediated, antibody-like interactions. The TCR adopted different docking modes on top of the prominently bulged peptide epitope in a TCR-pMHC 'superdimer'. Accordingly, there was no notable deformation of the prominent LPEP peptide, resulting in very limited MHC-mediated interactions. Hence, these interactions define the critically important sites on the MHC class I α1- and α2-helices that control MHC-restricted recognition by this TCR. Notably, although these sites demonstrated limited polymorphism, they represent conserved MHC class I contact points in almost all other reported TCR–pMHC-I structures, suggesting they are 'generic' docking points for MHC restriction.

RESULTS

Structure determination

We expressed and purified the HLA-B*3508–LPEP complex and the SB27 TCR as described[30]. We used crystals of the SB27–HLA-B*3508–LPEP complex to collect a 2.5-Å resolution data set (**Table 1**). The pseudo-orthorhombic crystals belonged to the space group $P2_1$ with unit cell dimensions of $a = 79.15$ Å, $b = 213.28$ Å, $c = 122.30$ Å and $\beta = 89.94°$, consistent with the presence of four TCR-pMHC complexes in the asymmetric unit. We refined the structure to R_{factor} and R_{free} values of 24.8% and 28.0%, respectively (**Table 1**). Although the individual TCR and pMHC components were almost identical, two TCR-pMHC complexes had distinct conformations (called 'complex A' and 'complex B' here). All TCR-pMHC complexes had well ordered electron density, and the electron density at the TCR-pMHC interface was unambiguous. The salient features of complex A are presented below first, followed by complex B for comparison.

The TCR–HLA-B*3508–LPEP complex

With respect to the long axis of the HLA-B*3508 peptide-binding groove, the SB27 TCR bound in an orthogonal mode (**Fig. 1**) distinct from the 'conserved diagonal footprint' used by other MHC class I–restricted TCRs. The SB27 TCR was positioned over the amino-terminal end of the antigen-binding cleft, where the V_α domain tilted toward the α2-helix such that the V_β domain formed very few interactions with the HLA-B*3508 heavy chain (**Figs. 1a** and **2a** and **Table 2**). The amino-terminal focus of pMHC recognition noted in SB27 is in contrast with that of the LC13–HLA-B8 nonamer complex, which interacts with the carboxy-terminal end of the pMHC complex[30] (**Fig. 2a**,**b**), suggesting that TCRs can potentially 'scan' pMHC surfaces to obtain optimal docking, rather than being rigidly constrained to focus on one or the other end of the MHC cleft[31,32]. The

Table 1 Data collection and refinement statistics for the SB27–HLA-B*3508–LPEP complex

Data collection	
Temperature (K)	100
X-ray source	BioCars, APS
Space group	$P2_1$
Cell dimensions (Å)	79.15, 213.28, 122.30, $\beta = 89.94°$
Resolution (Å)	2.5
Total observations	377,399
Unique observations	134,769
Multiplicity	2.8
Data completeness (%)	95.5 (97.6)
Data $> 2\sigma_I$ (%)	81.3 (53.2)
I / σ_I	12.98 (2.60)
R_{merge} (%)	8.7 (50.1)[a]
Refinement statistics	
Nonhydrogen atoms	
Protein	27,036
Water	239
Iodide	22
R_{factor} (%)[b]	24.8
R_{free} (%)[b]	28.0
r.m.s.d. from ideality	
Bond lengths (Å)	0.007
Bond angles (°)	0.989
Impropers (°)	1.22
Dihedrals (°)	27.9
Ramachandran plot	
Most favored	91.3
Allowed regions	8.7
B factors (Å²)[c]	
Average main chain	11.0
Average side chain	12.9
Average water molecule	18.3
r.m.s.d. bonded B factors	0.60, 2.01

Values in parentheses are for the shell of highest resolution.
[a] $R_{merge} = \Sigma|I_{hkl} - \langle I_{hkl}\rangle|/\Sigma I_{hkl}$.
[b] $R_{factor} = \Sigma_{hkl}||F_o| - |F_c||/\Sigma_{hkl}|F_o|$ for all data except 3%, which were used for R_{free} calculation.
[c] Residual B factors calculated by REFMAC (does not include the contribution to atomic displacements from translation, libration and screw-rotation displacement[62]).

SB27–HLA-B*3508–LPEP structure also shows that the bulged peptide does indeed act as a substantial hurdle to full engagement of the TCR with the HLA molecule. Despite the atypical binding, the affinity for the TCR-pMHC interaction[26] was well within the normal range noted for other TCRs (discussed below)[5,32]. The total buried surface area after binding between the TCR and MHC was about 1,900 Å^2, which is also in the range for TCR–pMHC-I structures that have already been determined[5]. The SB27 TCR made an unusually small number of contacts with the HLA-B*3508 heavy chain, with only 3 direct hydrogen bonds, 1 salt bridge and 46 van der Waals contacts, in contrast to the 13 direct hydrogen bonds and 91 van der Waals contacts for the LPEP peptide (complex A, **Table 2**). There were subtly different TCR-MHC contacts made in complex B, whereas the TCR-peptide contacts were much the same (**Supplementary Table 1** online). Accordingly, the LPEP peptide was particularly prominent in the buried surface area after TCR-pMHC binding (peptide, 45%, versus MHC, 55%), in contrast to typical TCR-pMHC structures[5], in which the peptide has been noted to

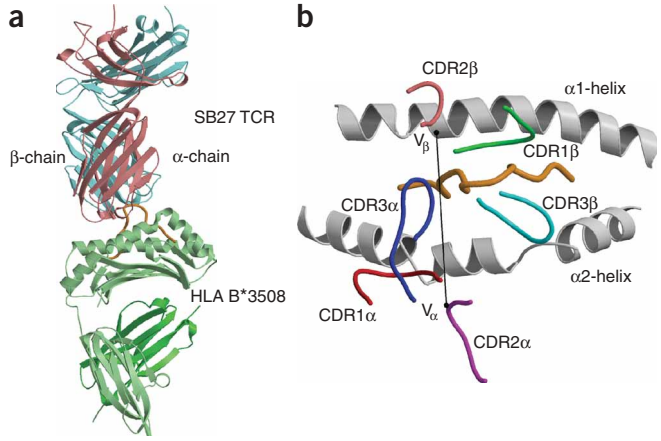

Figure 1 Overview of the SB27 TCR in complex with HLA-B*3508–LPEP. (**a**) SB27–HLA-B*3508–LPEP complex. SB27 TCR α-chain, light red; SB27 TCR β-chain, blue; HLA-B*3508 heavy chain, light green; HLA-B*3508 β_2-microglobulin domain, darker green; bound 13-residue epitope (LPEPLPQGQLTAY), orange. (**b**) The orthogonal mode of binding, viewed along the antigen-binding cleft. CDR loops: CDR1α, red; CDR2α, magenta; CDR3α, dark blue; CDR1β, green; CDR2β, pink; CDR3β, cyan. Black line indicates the centers of mass of the V_α and V_β domains.

contribute between 18% and 34% of the buried surface area after TCR-pMHC binding. For example, in the LC13–HLA-B8–FLR complex, the peptide contributes only 18% to the buried surface area after TCR-pMHC binding[30] (**Fig. 2**). Thus, the SB27 TCR is highly unusual in its pMHC-I interactions, adopting an orthogonal mode of binding and assuming a small MHC 'footprint' relative to that of other MHC class I–restricted TCRs.

Biased TCR gene usage

The CTL response to the LPEP epitope had limited TCR gene selection, with almost exclusive choice of TRBV5-6, TRBV6-1, TRBV7-2, TRBV20-1, TRBV27 or TRBV28 among the V_β chains used in three different HLA-B*3508 donors[26]. Notably, the choice of V_α regions and joining α-regions (J_α regions) was highly restricted, with TRAV19 and TRAJ34 found in nearly all clones in association with different TCR β-chains[26]. Moreover, despite multiple codon usage in the nontemplated nucleotide (N) regions of the V_α-J_α junctions, a conserved, nongermline Gly-Phe motif encoded at this site was present in nearly all CTL clones, indicating stringent selection for these residues in creating the HLA-B*3508–LPEP specificity. The fact that the SB27 TCR represents an archetypal clonotype of the HLA-B*3508–LPEP-specific repertoire (encoded by the TRAV19, TRAJ34, TRBV6-1 and TRBJ2-7 genes) allowed us to address the structural constraints determining these TCR biases.

There was an overall skewing toward pMHC contacts with the V_α domain buried surface area (58%) versus the V_β domain (42%) at the binding interface, providing an immediate clue to the structural basis for the restricted V_α gene usage (**Figs. 1b** and **2a** and **Table 2**). Reduced V_β usage at the TCR–pMHC-I interface has been noted before[33]. Complementarity-determining region-1α (CDR1α) contributed 10% of the buried surface area and CDR2α interacted almost exclusively with the MHC (14% buried surface area), whereas CDR3α had considerable involvement (34% buried surface area) in interacting with both the MHC and the peptide (**Fig. 2a** and **Table 2**). Collectively, the CDR1α, CDR2α and CDR3α loops of the V_α domain provided the main contacts with HLA-B*3508, forming a 'footprint' onto the α2-helix-spanning residues 150–158 (**Fig. 2a**). The CDR1α lay over the α2-helix of HLA-B*3508 but did not engage this region much, whereas the CDR2α loop lay peripheral to the α2-helix, yet made considerable contacts (**Fig. 2a**,**c**). Of note, Asn50α and Phe52α bridged the void between the TCR and the MHC (**Fig. 2c**). Phe52α 'packed against' Arg157, Glu154 and Ala158 of HLA-B*3508, whereas Asn50α made a hydrogen bond and van der Waals interaction with Glu154. Notably, neither Asn50α nor Phe52α was present in these positions for the CDR2α of any other V_α gene family sequence, reflecting the selective use of TRAV19 in the LPEP-specific CTL response.

The CDR3α loop 'sat' on the central axis of the antigen-binding cleft, making contacts with both the α-helices of the MHC and the peptide (**Figs. 1b** and **2a**,**c**). The fact that Gly94α of the conserved Gly-Phe motif from the V_α-J_α junctional N region did not contact the antigen indicates that its conservation reflects a structural function, as noted before for other TCRs[30,33,34]. However, Phe95α and the neighboring Tyr96α formed a focused contact site in which Phe95 interacted with Gln155 of HLA-B*3508 (**Fig. 2c**). Notably, the MHC residue Gln155 changed conformation upon TCR ligation. Before TCR ligation, Gln155 participates in a large network of water-mediated hydrogen bonds to the peptide[30,33,34]. After ligation, however, it swung around to interact with Phe95α and Leu98β while also

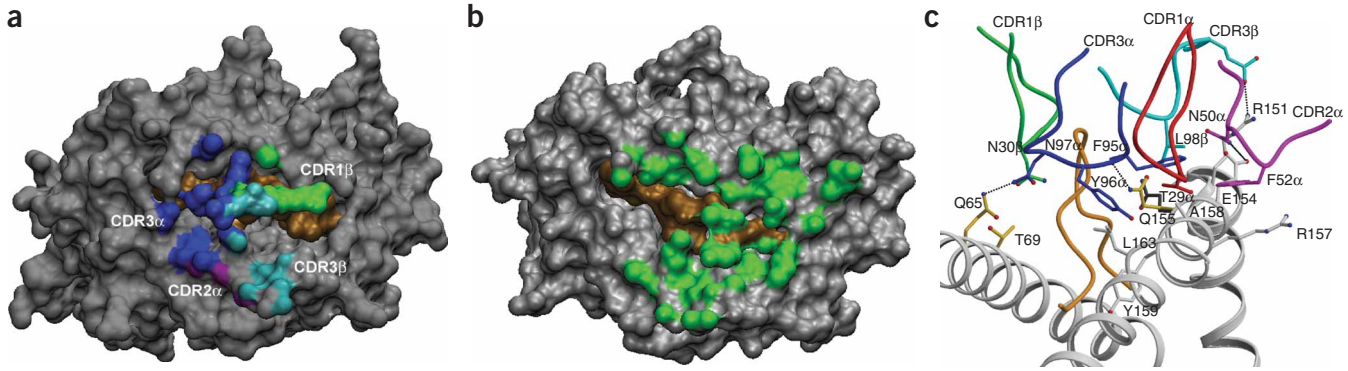

Figure 2 SB27 TCR contacts at the interface. (**a**) 'Footprint' of the SB27 TCR on the HLA-B*3508–LPEP complex. There are limited MHC-mediated contacts with the SB27 TCR on the gray surface representation of the HLA-B*3508 heavy chain. (**b**) 'Footprint' of the LC13 TCR in complex with HLA-B8–FLRGRAYGL, showing the focus toward the carboxy-terminal end of the peptide[5]. (**c**) Closer view of the SB27 TCR contacts with the HLA-B*3508–LPEP complex. HLA-B*3508 α-helices, light gray; peptide, orange; conformation of Gln155 as it appears in the binary complex (HLA-B*3508–LPEP)[3], dark gray; side chains from the triad of residues mediating MHC-restriction, gold. CDR loop colors are as in **Figure 1b**.

Table 2 Contacts at the TCR-pMHC interface and the genetic origin of TCR residues

	SB27 TCR	MHC	Type of bond	Contacts	TCR gene segment
CDR1α	Thr29	Ala158	VDW	5	V_α
CDR2α	Asn50	Glu154	VDW	3	V_α
	$Asn50^{N\delta2}$	$Glu154^{O\varepsilon2}$	H bond	1	V_α
	Phe52	Glu154, Ala158, Arg157	VDW	5	V_α
CDR3α	Phe95	Gln155, Ala158	VDW	12	N region
	$Phe95^{O}$	$Gln155^{N\varepsilon2}$	H bond	1	N region
	Tyr96	Leu163, Ala158,Tyr159, Gln155	VDW	10	J_α
	Asn97	Gln65	VDW	2	J_α
	$Asn97^{N\delta2}$	$Gln65^{N\varepsilon2}$	H bond	1	J_α
CDR1β	Asn30	Thr69	VDW	1	V_β
CDR2β	Ser51	Gln65	VDW	1	V_β
CDR3β	Leu98	Arg151, Ala150, Gln155, Glu154	VDW	7	D_β-N
	$Glu101^{O\varepsilon1}$	$Arg151^{NH1}$	Salt bridge	1	N-J_β
	SB27 TCR	Peptide			
CDR1α	Tyr31	Gln7	VDW	3	V_α
	$Tyr31^{O\eta}$	$Gln7^{O\varepsilon1}$	H bond	1	V_α
CDR3α	Ser93	Gln7	VDW	1	V_α
	Ser93	$Gln7^{O\varepsilon1,N\varepsilon2}$	Two H bonds	2	V_α
	Gly94	Gln7	VDW	3	N region[a]
	Phe95	Pro6, Gln7	VDW	2	N region
	Tyr96	Leu5, Pro4, Gln7	VDW	15	J_α
	$Asn97^{N,O\delta1}$	$Leu5^{O}$	Two H bonds	2	J_α
	Asn97	Leu5, Pro6, Gln7	VDW	13	J_α
	Asp102	Gln7	VDW	1	J_α
CDR1β	Met27	Gln9	VDW	4	V_β
	Asn28	Gln9	VDW	9	V_β
	$Asn28^{O\delta1}$	$Gln9^{N\varepsilon2}$	H bond	1	V_β
	$His29^{N\delta1}$	$Gln9^{N}$	H bond	1	V_β
	His29	Gly8, Gln7, Gln9	VDW	12	V_β
	$Asn30^{N}$	$Gln7^{O}$, $Gly8^{O}$	Two H bonds	2	V_β
	Asn30	Leu5, Gln7, Pro6, Gly8, Leu10	VDW	12	V_β
	$Asn30^{N\delta2}$	$Pro6^{O}$, $Gly8^{O}$	Two H bonds	2	V_β
	$Ser31^{N}$	$Gln7^{O}$	H bond	1	V_β
	Ser31	Gln7	VDW	5	V_β
	$Tyr33^{O\eta}$	$Gln7^{N\varepsilon2}$	H bond	1	V_β
	Tyr33	Gln7	VDW	3	V_β
CDR3β	Pro95	Gln7, Gly8	VDW	8	D_β-N

Water-mediated TCR-peptide interactions

	TCR	Peptide	Type
CDR3β	$Ser94^{O\gamma}$, $Pro95^{O}$	$Gln7^{O}$	H bond
CDR1β	$Ser31^{O}$	$Gln7^{O}$	H bond

Water-mediated TCR-MHC interactions

	TCR	MHC	Type
CDR3α	$Tyr96^{O\eta}$, $Thr29^{O\eta}$	$Leu163^{N}$, $Ala158^{O}$	H bond

The SB27 TCR designation is TRBV6-1, TRBD indeterminate, TRBJ2-7, TRAV19 and TRAJ34 according to the nomenclature of the IMGT (the international ImMunoGeneTics database). [a]TRAV19 has undergone remodeling of the V_α exon encoding the carboxy-terminal end of V_α at the V-J junction, creating the amino acid sequence CALSG instead of the germline sequence CALSE[66]. Superscripted designations indicate element involved in hydrogen bonding. H bond, hydrogen bond; VDW, van der Waals.

forming a hydrogen bond to the main chain of Phe95 (**Fig. 2c**). This multifunctional switching of Gln155 interactions between peptide and TCR has been noted before[30], suggesting that this residue may act as a 'gatekeeper', guiding MHC class I–restricted T cell recognition.

In the V_β domain, CDR1β (20% total buried surface area) interacted prominently with the peptide; CDR3β contributed 19% to the interface, whereas CDR2β contributed only minimally (3% buried surface area). The V_β domain made substantial interactions with the peptide (**Fig. 2a**), consistent with the biased selection of certain V_β regions in this LPEP-specific CTL response. In comparison, the V_β domain interacted minimally with the MHC (**Table 2** and **Fig. 2a,c**). The CDR3β loop made two of these interactions via

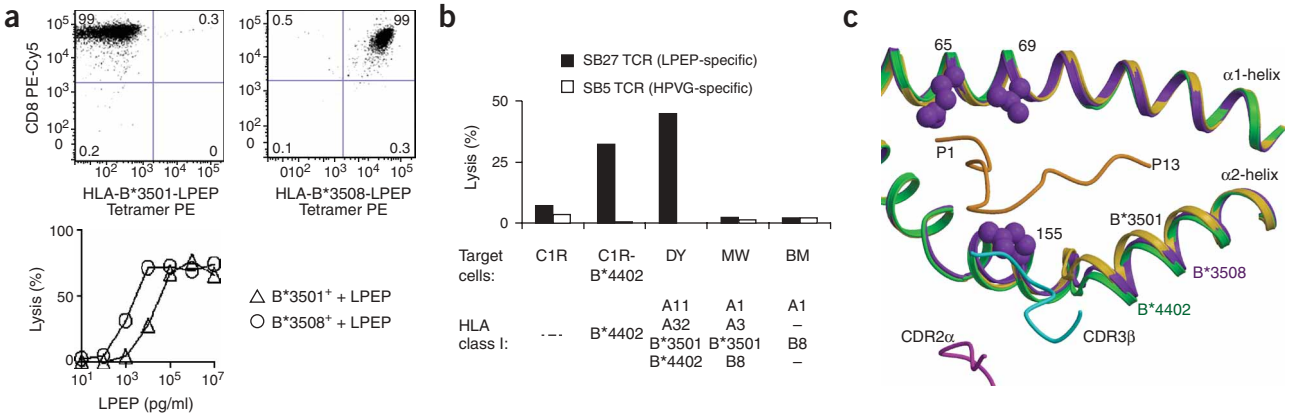

Figure 3 The SB27 CTL clone is both MHC restricted and alloreactive with HLA-B*4402, with which it shares structural features in the region of the TCR footprint. (**a**) Top, staining of the SB27 CTL clone with antibody to CD8 and an HLA-B*3501–LPEPLPQGQLTAY or HLA-B*3508–LPEPLPQGQLTAY pentameric complex. Numbers in corners indicate percentage of cells in that quadrant. PE, phycoerythrin; Cy5, indodicarbocyanine. Bottom, peptide dose-response cytotoxicity assays with the SB27 CTL clone, the LPEPLPQGQLTAY peptide, and either HLA-B*3501+ or HLA-B*3508+ phytohemagglutinin blast target cells. Data are representative of two independent experiments with similar results. (**b**) Specific lysis by SB27 CTLs of target cells positive or negative for HLA-B*4402 expression, including the HLA class I–negative mutant cell line C1R that was transfected with a plasmid containing cDNA encoding the HLA-B*4402 molecule (C1R-B*4402). SB5, CTL clone that recognizes another Epstein-Barr virus epitope (specific for HPVGEADYFEY-HLA-B*3508; negative control). DY, MW and BM, cell lines. Data are representative of two independent experiments with similar results. (**c**) SB27 TCR MHC class I docking sites on the α1- and α2-helices of HLA-B*3508–LPEP (purple), HLA-B*3501–LPEP (orange) and an HLA-B*4402–nonamer complex (green)[5]. The triad of residues that mediate MHC restriction are in purple.

Glu101β and Leu98β, both encoded by the nongermline, remodeled diversity β-region (D_β)–N-J segment. Leu98β from the CDR3β loop formed many van der Waals interactions, nestling between the long aliphatic side chains of Gln155 and Arg151, whereas Glu101β made a salt bridge to Arg151 on the α2-helix of HLA-B*3508. The other V_β contacts (discussed below) involved Ser51β from the CDR2β loop and Asn30β from the CDR1β loop. These findings provide a structural basis for the highly constrained αβ TCR repertoire restricted toward the HLA-B*3508–LPEP complex.

MHC-restricted recognition

Given that the SB27 TCR 'struggles' to contact HLA-B*3508, what does this atypical complex indicate about the structural features of MHC class I that mediate generic mechanisms of MHC-restriction[4]? The SB27 TCR interacted with only two residues on the HLA-B*3508 α1-helix, Gln65 and Thr69: Asn30β formed van der Waals contact with Thr69, whereas Asn97α formed a hydrogen bond to Gln65, which also made van der Waals interactions with Ser51β (**Fig. 2c**). Despite their limited polymorphism, these two positions are involved in TCR-mediated contacts in almost all the TCR–pMHC-I structures determined so far[9,30,33,35–40]. Moreover, alanine-scanning mutagenesis has also shown that these two positions (and α1-helix residue 66) represent energetic 'hotspots' in two different TCR–pMHC systems[41–43]. Accordingly, positions 65 and 69 seem to represent a 'generic' MHC class I restriction element.

Moreover, the SB27 TCR is exquisitely MHC restricted in its antigen recognition in that the single-residue polymorphism that distinguishes HLA-B*3501 (Leu156) from HLA-B*3508 (Arg156) resulted in a loss of staining of the SB27 T cells with B*3501–LPEP pentamers (**Fig. 3a**). This polymorphism also considerably impaired SB27 recognition of B*3501 targets; approximately tenfold more LPEP peptide was required for equivalent killing of HLA-B*3508 targets (**Fig. 3a**). Surface plasmon resonance binding studies were also consistent with restriction of the SB27 TCR to HLA-B*3508, as the HLA-B*3508–LPEP complex bound the SB27 TCR with higher affinity (K_d = 9.9 μM) than the HLA-B*3501–LPEP complex (K_d = 35.2 μM)[26]. These observations collectively define the 'binding window' for MHC restriction and productive CTL recognition of the HLA-B*3508–LPEP versus HLA-B*3501–LPEP complexes. Notably, however, when tested for CTL lysis of a panel of allogeneic cells without exogenous peptide addition, the SB27 CTL clone was crossreactive with the allogeneic class I molecule HLA-B*4402 (**Fig. 3b**). Although the structural basis of T cell alloreactivity is not completely known, recognition of allogeneic MHC class I is thought to involve interactions with a mixture of residues from the MHC and endogenous peptide and is considered to reflect a bias of thymically selected TCRs toward recognition of pMHC. Hence, despite 21–amino acid differences between HLA-B*3508 and HLA-B*4402 (16 of which are located in the α1- and α2-domains), the MHC class I residues forming the 'footprint' of SB27 on HLA-B*3508 (Gln65, Thr69, Ala150, Arg151, Glu154 and Gln155) were all present in HLA-B*4402, suggesting a shared docking mode that dictates this alloreactive recognition (**Fig. 3c**). The alloreactivity of SB27 is typical of other MHC class I–restricted, antiviral CTLs that recognize peptides of canonical length[26].

The structural basis for restricted SB27 recognition of HLA-B*3508 versus HLA-B*3501 was not the result of differences in the conformation of the LPEP peptide bound to these two allotypes, as these conformations are essentially identical[26]. Accordingly, the TCR discrimination of HLA-B*3508 and HLA-B*3501–LPEP complexes rested mainly with the rigid body shift (spanning residues 145–158) in the α2-helix in the B*3508–LPEP complex. This MHC class I alteration broadened the antigen-binding cleft of HLA-B*3508 compared with that of HLA-B*3501 (ref. 26), thereby favoring TCR interaction with HLA-B*3508. Notably, this region corresponded to the SB27 'footprint' on HLA-B*3508, where it made contacts with α2-helix residues 150, 151, 154 and 155 (**Table 2**) and also shared close similarity with the corresponding part of the α2-helix of HLA-B*4402 (ref. 44; **Fig. 3c**). However, the narrower antigen-binding cleft in this region of HLA-B*3501 would result in a sterically

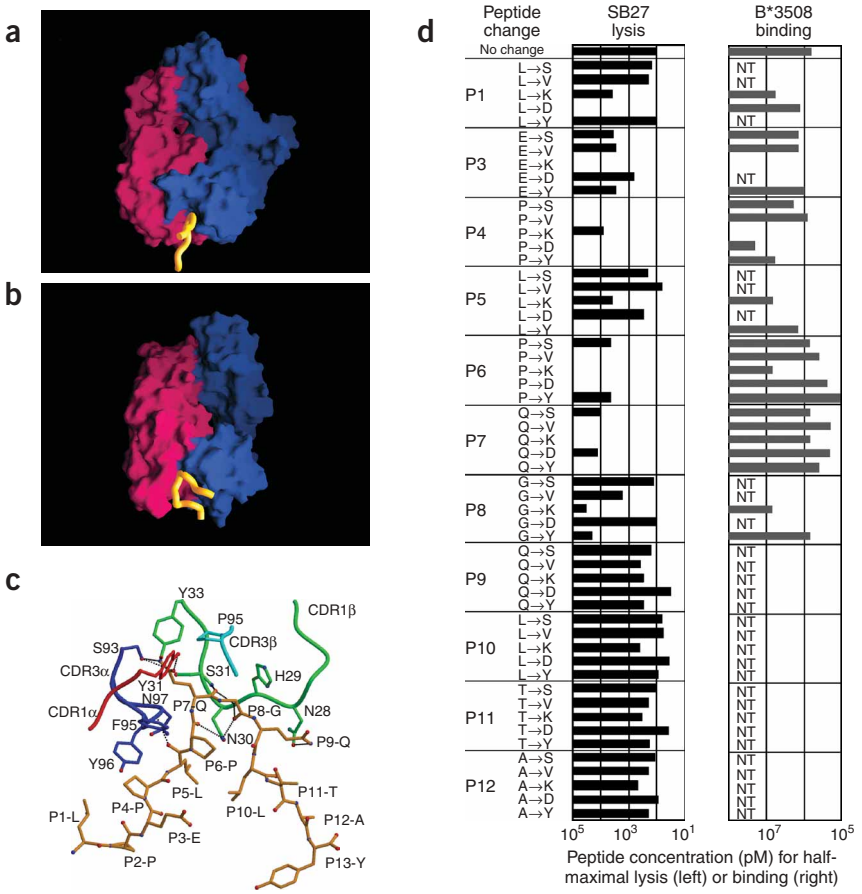

Figure 4 SB27 TCR recognition of the HLA-B*3508–LPEP complex is antibody like and is dominated by TCR-peptide interactions. (**a**,**b**) GRASP image of the SB27 TCR-peptide interaction (**a**) compared with that of a complex between an Fab and a peptide from human rhinovirus viral capsid protein VP2 (**b**; Protein Data Bank accession number, 1A3R)[46]. TCR V_α and Fab V_H, red; TCR Vβ and Fab V_L, blue; Epstein-Barr virus LPEP and rhinovirus VP2 peptides, yellow. (**c**) Closer view of the SB27 TCR interactions with the solvent-exposed side chains of the LPEP peptide. Peptide, orange; CDR loop colors are as in **Figure 1b**. (**d**) Dose-response assays of analogs of the 13-residue peptide (LPEPLPQGQLTAY) that include single–amino acid substitutions, assessing recognition by SB27 CTLs (chromium-release assays, left) and binding to 'empty' HLA-B*3508 with the transporter associated with antigen processing–deficient T2-B*3508 (right). Peptides recognized well in the cytotoxicity assays are assumed to bind well to HLA-B*3508 and are therefore excluded from the MHC-binding assays (NT). Data represent peptide concentrations for half-maximal lysis or binding calculated from dose-response curves for each peptide and are representative of two independent experiments with similar results.

unfavorable 'clash' between Arg151 of HLA-B*3501 and CDR3β, which is also likely to disrupt the hydrogen bond between the TCR Asn50α and the MHC class I Glu154. In analysis of the available TCR–pMHC-I α2-helix interactions, position 155 represents the only MHC position that has a conserved function in interacting with the TCR that might potentially be preserved in the lower-affinity interaction between HLA-B*3501–LPEP and SB27. Thus, constraints imposed by the bulged peptide in this complex have considerably limited the number of TCR-MHC contacts and shed light on the minimal requirements for MHC-restriction.

TCR interaction with the bulged epitope

The mode of interaction of the SB27 TCR with the prominent bulged epitope has not been reported before to our knowledge in αβ TCR recognition, but it is reminiscent of antibody-mediated recognition of proteins[45] and peptide antigens[46] (**Fig. 4a–c**). The LPEP peptide contributed twice as many contacts with the TCR interface as the MHC (**Table 2**). Whereas one to three peptide residues from most pMHC ligands interact with the TCR[5], seven peptide side chains from the HLA-B*3508–LPEP complex interacted with SB27. Nonetheless, the free LPEP peptide did not bind the SB27 TCR directly, because high concentrations of peptide did not inhibit TCR recognition of the HLA-B*3508–LPEP complex on antigen-presenting cells (data not shown). The buried surface area of the TCR-peptide was 855 $Å^2$, which is very similar to that of antibody-antigen interactions[45], including Fab′-peptide complexes[46]. The bulged region of the epitope was not deformed by TCR ligation, but instead became walled by CDR3α, which interacted with the amino-terminal slope of the peptide (**Figs. 2a**,**c** and **4c**). CDR3β crossed over the tip of the bulged epitope, whereas CDR1β ran approximately antiparallel to the bulged region (**Fig. 4c**). All the residues in the CDR1β loop were prominent in recognition of the peptide in this highly unusual arrangement. However, among the different V_β segments used in the response to the HLA-B*3508–LPEP, the germline-encoded CDR1β sequences varied substantially, preventing any firm conclusions regarding the structural basis for their biased selection. Residues 4–9 of the peptide interacted directly with the TCR, whereas Leu at position 10 made a water-mediated interaction (**Table 2**). Hence, Thr at position 11 was the only surface-exposed residue that did not interact with the TCR (**Fig. 4c**). These results are consistent with the substantial loss of CTL activity after substitution of residues at positions 4–8 with other amino acids that do not affect MHC binding[26] (**Fig. 4d**). The relative insensitivity of CTL recognition to substitutions at positions 9, 10 and 11 was consistent with their minimal or lack of involvement in making TCR contacts (**Fig. 4c** and **Table 2**). The small side chain of the Gly at position 8 allowed the Gln at position 7 to protrude deeply into a pocket in the SB27 TCR binding surface such that this Gln side chain formed hydrogen bonds with CDR1α Tyr31α and Ser93α. It is not certain that this pocket exists in the TCR not in complex, but it represents another antibody-like feature of antigen recognition by the SB27 TCR.

Alternative docking modes of the TCR

There was a TCR-pMHC dimer present in the crystal lattice (complexes A and B; **Fig. 5a**). Superimposition of complexes A and B showed that the SB27 TCR adopted two different docking

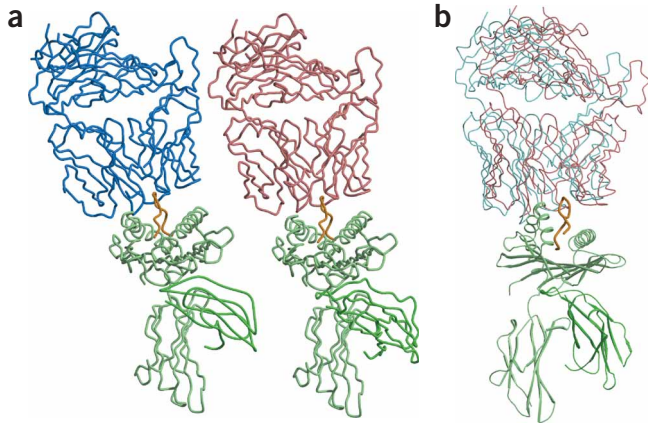

Figure 5 The SB27 TCR–HLA-B*3508–LPEP complex forms a TCR 'superdimer' with two subtly different TCR–pMHC-I orientations. (**a**) The 'superdimer' of the TCRs. TCR of complex A, red; TCR of complex B, blue; MHC, green; peptide, yellow. (**b**) Superimposition of the two orientations of the TCR to demonstrate the 12° rotation of one complex relative to the other.

strategies that differed by 12°. This rotation axis was parallel to the peptide-binding groove, causing atomic shifts in excess of 7 Å, resulting in leaning of the TCR more toward the α2-helix of the MHC (**Fig. 5b**). Such differential docking resulted in a few more contacts mediated by the α2-helix in complex B (**Supplementary Table 1** online), mainly by means of the CDR1α loop (the buried surface area contribution increased from 10% to 15% in the two complexes). In addition, the increased contacts included a salt bridge between Asp53α and Arg157. However, because of the loss of other contacts, there was no net increase in the buried surface area between the complexes. Although the peptide-mediated contacts were mostly conserved, there was clearly increased mobility of the noncontacting region in the CDR3β loop. The structure of the γδ TCR G8 has shown potentially functional TCR dimerization that might provide a mechanism for the TCR oligomerization[47] that is known to be essential for T cell signaling and activation[32,48]. The dimer interface of the G8 γδ TCR involves an extensive hydrogen-bonding network between the 'a' strands of the V_δ domains. In contrast, the dimerization of SB27 is mediated by seven hydrogen bonds involving residues from the constant α-region (C_α), C_β, V_α and V_β domains. The TCR oligomerization may represent a crystal artifact, however, as we did not find TCR dimers in solution by size-exclusion chromatography. Nevertheless, TCR-pMHC 'superdimers' may potentially be relevant after coreceptor recruitment or the higher-order arrangement of molecules in the immunological synapse in the context of the crowded cell surface.

DISCUSSION

Noncanonical, longer peptides are important in MHC class I–restricted immunity, yet the mechanism of TCR binding to these peptides has remained an enigma because they expose many more side chains than usual and their bulging from the MHC class I cleft poses a steric challenge to MHC-restricted αβ T cell recognition. The SB27 αβ TCR engaged a rigid, 'superbulged' epitope bound to HLA-B*3508 by adopting an orthogonal binding mode, thus challenging previous generalizations regarding MHC class–specific modes of recognition[7,8,32]. Despite the limited MHC contacts, the recognition of SB27 remained MHC restricted and provides insights into the minimal requirements for MHC restriction; that is, positions 65 and 69 on the α1-helix and 155 on the α2-helix. Position 155 seems to act as a 'gatekeeper' residue, switching upon TCR ligation from stabilizing the peptide to interacting with the TCR. Given this minimal 'restriction triad', it seems likely that coreceptors must provide a guiding function in TCR-pMHC recognition[49], as demonstrated by their involvement in the immunological synapse and supported by finding that T cells can respond to a single molecule of specific pMHC ligand[50–52].

The limited MHC-mediated contacts noted in the SB27–HLA-B*3508–LPEP complex are also consistent with published findings[7,41,43]. That is, despite many MHC-mediated contacts in an extensive TCR-pMHC interface, it seems that only a limited number of MHC residues have an essential energetic function in mediating ligation. For example, in the LC13–HLA-B8–FLR complex, positions 65, 66, 69, 72 from the α1-helix and 146, 150 and 155 from the α2-helix have been suggested as likely energetic 'hotspots', whereas in the A6–HLA-A2–Tax complex, positions 65, 66 and 69 from the α1-helix have been suggested as crucial interaction sites. These energetic 'hotspots', as noted in other receptor systems[53,54], seem to dictate the interaction between the αβ TCR and pMHC-I.

Our findings document a much more extensive role for TCR-peptide interactions than reported so far for other TCR-pMHC complexes. The complex formed a TCR-pMHC 'superdimer' with two distinct docking orientations, as if the TCR might 'see-saw' back and forth on the prominent epitope, emphasizing the scanning function of the TCR and the finely balanced nature of SB27 MHC restriction. Notably, the minimal 'generic footprint' was preserved in both docking orientations. The exaggerated function of the LPEP epitope in mediating interactions with the SB27 TCR is reminiscent of the 'peptidic-self' model of MHC-restriction. This early theory of T cell recognition suggested that TCRs interact mainly or exclusively with peptide antigen and that MHC restriction is a consequence of the orientation of peptide antigen by the polymorphic MHC molecules[55]. This is not the case with the MHC-restricted recognition of the HLA-B*3508–LPEP complex by the SB27 TCR, in which despite the antibody-like TCR recognition of the bulged peptide, we found a minimal structural basis for MHC restriction through TCR interaction with relatively conserved MHC class I residues. This observation suggests an inherent mechanism that determines TCR bias toward the recognition of MHC class I molecules.

METHODS

Protein expression, purification and crystallization. The HLA-B*3508–LPEP complex[26] and the SB27 TCR were expressed and purified as described[56,57]. Crystals of the SB27–HLA-B*3508–LPEP complex were formed at 4 °C with the hanging-drop vapor-diffusion technique, in which an equal volume of SB27–HLA-B*3508–LPEP (10 mg/ml) was mixed with the reservoir (200 mM potassium iodide, 16% PEG 3350 and 100 mM cacodylate, pH 6.7).

Data collection, structure determination and refinement. Crystals were directly transferred to cryoprotectant containing 20% glycerol and were 'flash-frozen' before data collection. Data were collected on an in-house radiation source and at Advanced Photon Source and were processed and scaled with the HKL2000 (ref. 58) suite (**Table 1**). Crystals were initially assigned to the space group $P2_12_12$, with a solvent content consistent with two TCR-pMHC complexes per asymmetric unit.

The structure was determined with the molecular replacement method, as implemented by the PHASER program[59], although the structure determination was nontrivial. The crystals were pseudo-orthorhombic and actually belonged to the space group $P2_1$ with the unit cell dimensions $a = 79.15$ Å, $b = 213.28$ Å, $c = 122.30$ Å, $\beta = 89.94°$, consistent with the presence of four TCR-pMHC complexes in the asymmetric unit. Using individual superposed ensembles of pMHC-I and TCR structures, we were able to locate two TCR-pMHC class I

complexes in the asymmetric unit. After that, we were able to further locate two additional MHC molecules in the asymmetric unit. However, there were substantial 'clashes' between the TCRs when the four TCR-pMHC class I complexes were assumed to be identical. Unbiased features of the electron density maps suggested that the two remaining TCRs to be located were not identical in their docking relative to the pMHC-I. The TCRs in these two complexes (A and B) are rotated 12° with respect to each other.

Unbiased features in the initial electron density map confirmed the correctness of the molecular replacement solution. The progress of refinement was monitored by the R_{free} value (3% of the data) with neither a sigma nor a low-resolution cutoff being applied to the data. The structure was initially refined with rigid-body fitting of the individual domains to a resolution of 4 Å, which led to an R_{free} value of 38.9%. Maximum likelihood refinement followed, as implemented in the REFMAC program[60], interspersed with rounds of model building with the 'O' program[61]. Tightly restrained individual B-factor refinement was used, and bulk solvent corrections were applied to the data set. Tight noncrystallographic symmetry restraints were used throughout the refinement, unless deviations from noncrystallographic symmetry were noted, and translation, libration and screw-rotation displacement refinement[62] was used to model anisotropic displacements of defined domains. Water molecules were included in the model if they were within hydrogen-bonding distance to chemically reasonable groups, appeared in $F_o - F_c$ maps contoured at 3.5 σ and had a B-factor of less than 80 Å^2. With these criteria, 239 water molecules were added. **Table 1** presents the final refinement and model statistics and **Supplementary Table 1** online presents a detailed description of TCR contacts with the HLA-B*3508 heavy chain and LPEP peptide in complex B.

Cell lines. Cells of a B lymphoblastoid line were established by exogenous transformation of peripheral B cells with Epstein-Barr virus derived from the supernatant of the B95.8 cell line and were maintained in growth medium (10% FCS in RPMI 1640 medium). The mutant B lymphoblastoid cell line × T lymphoblastoid hybrid cell line 174 × CEM.T2 (called 'T2' here)[63] expressing HLA-B*3508 (T2.B*3508) was also used and has been described[25]. The Hmy2.C1R mutant B lymphoblastoid cell line was also used. This line was generated by irradiation of the fast-growing lymphoma LICR.LON.Hmy2 and selection with antibodies to HLA-A and HLA-B alleles and complement. This resulted in a cell line with no detectable HLA-A or HLA-B gene products but with intact antigen-processing and antigen-presentation pathways[64]. Thus, these cells were able to support high expression of individually transfected HLA-A, HLA-B or HLA-C gene products[64]. HLA-B*4402 was transfected into C1R by electroporation (975 F and 200 V) with a plasmid containing cDNA encoding the HLA-B*4402 molecule and a selectable marker (pREP7) at a ratio 10:1. Phytohemagglutinin blasts were generated as described[65]. CTL clones were generated by agar cloning as described[26].

Cytotoxicity assay. CTL clones were tested in duplicate in the standard 5-hour chromium-release assay for cytotoxicity against ^{51}Cr-labeled target cells, some of which had been treated for 1 h with various concentrations of peptide. The percent specific lysis was calculated, and the peptide concentration required for half-maximum lysis was determined from dose-response curves. Peptides were synthesized by Mimotopes. A β-scintillation counter (Topcount Microplate; Packard Instruments) was used to measure ^{51}Cr in assay supernatant samples. The mean spontaneous lysis for target cells in culture medium was always less than 20%, and variation about the mean specific lysis was less than 10%.

Cell staining and HLA class I peptide-binding assays. For assessment of staining, the SB27 clone was incubated for 30 min at 4 °C with an HLA-B*3508-LPEP, phycoerythrin-labeled pentamer or with an HLA-B*3501–LPEP, phycoerythrin-labeled pentamer (ProImmune). Cells were then washed twice and labeled for 30 min at 4 °C with Tricolor-labeled antibody to human CD8 (Caltag). Cells were again washed and analyzed on a FACSCanto with FACSDiva software (Becton Dickinson).

For assessment of peptide binding to HLA-B*3508, T2.B*3508 cells were incubated at 26 °C for 14–16 h in AIM V serum-free medium (Invitrogen) with various concentrations (0.01, 0.1, 1, 10 and 100 μM) of peptides, followed by incubation at 37 °C for 2–3 h and staining for HLA-B35 surface expression. HLA-B35 surface expression was measured by flow cytometry on a FACSCalibur (Becton Dickinson) with a monoclonal antibody to HLA-Bw6 (SFR8 Bw6).

Accession codes. Protein Data Bank: structures and translation, libration and screw-rotation displacement parameters, 2AK4.

Note: Supplementary information is available on the Nature Immunology website.

ACKNOWLEDGMENTS

We thank A. Brooks and D. El-hassen for discussions and reagents; P. Doherty, F. Carbone and S. Turner for critical reading of the manuscript; and the BioCars staff for assistance in data collection at Advanced Photon Source (Chicago, Illinois). J.R. and J.M. are joint senior authors. Supported by the National Health and Medical Research Council Australia, Roche Organ Transplantation Research Fund, Australian Research Council, National Health and Medical Research Council Career Development Award (S.B.), National Health and Medical Research Council Peter Doherty Training Fellowship (T.B.) and Wellcome Trust (J.R.).

COMPETING INTERESTS STATEMENT

The authors declare that they have no competing financial interests.

Published online at http://www.nature.com/natureimmunology/
Reprints and permissions information is available online at http://npg.nature.com/reprintsandpermissions/

1. Townsend, A. & Bodmer, H. Antigen recognition by class I-restricted T lymphocytes. *Annu. Rev. Immunol.* **7**, 601–624 (1989).
2. Rammensee, H.G., Falk, K. & Rotzschke, O. Peptides naturally presented by MHC class I molecules. *Annu. Rev. Immunol.* **11**, 213–244 (1993).
3. Zinkernagel, R.M. & Doherty, P.C. Restriction of in vitro T cell-mediated cytotoxicity in lymphocytic choriomeningitis within a syngeneic or semiallogeneic system. *Nature* **248**, 701–702 (1974).
4. Garboczi, D.N. & Biddison, W.E. Shapes of MHC restriction. *Immunity* **10**, 1–7 (1999).
5. Rudolph, M.G. & Wilson, I.A. The specificity of TCR/pMHC interaction. *Curr. Opin. Immunol.* **14**, 52–65 (2002).
6. van der Merwe, P.A. & Davis, S.J. Molecular interactions mediating T cell antigen recognition. *Annu. Rev. Immunol.* **21**, 659–684 (2003).
7. Wu, L.C., Tuot, D.S., Lyons, D.S., Garcia, K.C. & Davis, M.M. Two-step binding mechanism for T-cell receptor recognition of peptide MHC. *Nature* **418**, 552–556 (2002).
8. Reinherz, E.L. *et al.* The crystal structure of a T cell receptor in complex with peptide and MHC class II. *Science* **286**, 1913–1921 (1999).
9. Stewart-Jones, G.B., McMichael, A.J., Bell, J.I., Stuart, D.I. & Jones, E.Y. A structural basis for immunodominant human T cell receptor recognition. *Nat. Immunol.* **4**, 657–663 (2003).
10. Hahn, M., Nicholson, M.J., Pyrdol, J. & Wucherpfennig, K.W. Unconventional topology of self peptide-major histocompatibility complex binding by a human autoimmune T cell receptor. *Nat. Immunol.* **6**, 490–496 (2005).
11. Fremont, D.H., Matsumura, M., Stura, E.A., Peterson, P.A. & Wilson, I.A. Crystal structures of two viral peptides in complex with murine MHC class I H-2Kb. *Science* **257**, 919–927 (1992).
12. Madden, D.R., Garboczi, D.N. & Wiley, D.C. The antigenic identity of peptide-MHC complexes: a comparison of the conformations of five viral peptides presented by HLA-A2. *Cell* **75**, 693–708 (1993).
13. Zhang, W., Young, A.C., Imarai, M., Nathenson, S.G. & Sacchettini, J.C. Crystal structure of the major histocompatibility complex class I H-2K^b molecule containing a single viral peptide: implications for peptide binding and T-cell receptor recognition. *Proc. Natl. Acad. Sci. USA* **89**, 8403–8407 (1992).
14. Goldberg, A.L., Cascio, P., Saric, T. & Rock, K.L. The importance of the proteasome and subsequent proteolytic steps in the generation of antigenic peptides. *Mol. Immunol.* **39**, 147–164 (2002).
15. Momburg, F., Neefjes, J.J. & Hammerling, G.J. Peptide selection by MHC-encoded TAP transporters. *Curr. Opin. Immunol.* **6**, 32–37 (1994).
16. Fruci, D. *et al.* Quantifying recruitment of cytosolic peptides for HLA class I presentation: impact of TAP transport. *J. Immunol.* **170**, 2977–2984 (2003).
17. Serwold, T., Gonzalez, F., Kim, J., Jacob, R. & Shastri, N. ERAAP customizes peptides for MHC class I molecules in the endoplasmic reticulum. *Nature* **419**, 480–483 (2002).
18. York, I.A. *et al.* The ER aminopeptidase ERAP1 enhances or limits antigen presentation by trimming epitopes to 8–9 residues. *Nat. Immunol.* **3**, 1177–1184 (2002).
19. Horig, H., Young, A.C., Papadopoulos, N.J., DiLorenzo, T.P. & Nathenson, S.G. Binding of longer peptides to the H-2K^b heterodimer is restricted to peptides extended at their C terminus: refinement of the inherent MHC class I peptide binding criteria. *J. Immunol.* **163**, 4434–4441 (1999).
20. Guo, H.C. *et al.* Different length peptides bind to HLA-Aw68 similarly at their ends but bulge out in the middle. *Nature* **360**, 364–366 (1992).
21. Chen, Y. *et al.* Naturally processed peptides longer than nine amino acid residues bind to the class I MHC molecule HLA-A2.1 with high affinity and in different conformations. *J. Immunol.* **152**, 2874–2881 (1994).
22. Urban, R.G. *et al.* A subset of HLA-B27 molecules contains peptides much longer than nonamers. *Proc. Natl. Acad. Sci. USA* **91**, 1534–1538 (1994).

23. Speir, J.A., Stevens, J., Joly, E., Butcher, G.W. & Wilson, I.A. Two different, highly Exposed, bulged structures for an unusually long peptide bound to rat MHC class I RT1-Aa. *Immunity* **14**, 81–92 (2001).
24. Probst-Kepper, M. *et al.* Conformational restraints and flexibility of 14-meric peptides in complex with HLA-B*3501. *J. Immunol.* **173**, 5610–5616 (2004).
25. Green, K.J. *et al.* Potent T cell response to a class I-binding 13-mer viral epitope and the influence of HLA micropolymorphism in controlling epitope length. *Eur. J. Immunol.* **34**, 2510–2519 (2004).
26. Tynan, F.E. *et al.* High resolution structures of highly bulged viral epitopes bound to major histocompatibility complex class I: implications for T-cell receptor engagement and T-cell immunodominance. *J. Biol. Chem.* **280**, 23900–23909 (2005).
27. Collins, E., Garboczi, D., Karpusas, M. & Wiley, D. The three-dimensional structure of a class I major histocompatibility complex molecule missing the α3 domain of the heavy chain. *Proc. Natl. Acad. Sci. USA* **92**, 1218–1221 (1995).
28. Zavala-Ruiz, Z., Strug, I., Walker, B.D., Norris, P.J. & Stern, L.J. A hairpin turn in a class II MHC-bound peptide orients residues outside the binding groove for T cell recognition. *Proc. Natl. Acad. Sci. USA* **101**, 13279–13284 (2004).
29. Probst-Kepper, M. *et al.* An alternative open reading frame of the human macrophage colony-stimulating factor gene is independently translated and codes for an antigenic peptide of 14 amino acids recognized by tumor-infiltrating CD8 T lymphocytes. *J. Exp. Med.* **193**, 1189–1198 (2001).
30. Kjer-Nielsen, L. *et al.* A structural basis for the selection of dominant $\alpha\beta$ T cell receptors in antiviral immunity. *Immunity* **18**, 53–64 (2003).
31. Garcia, K.C., Teyton, L. & Wilson, I.A. Structural basis of T cell recognition. *Annu. Rev. Immunol.* **17**, 369–397 (1999).
32. Krogsgaard, M. & Davis, M.M. How T cells 'see' antigen. *Nat. Immunol.* **6**, 239–245 (2005).
33. Ding, Y.H. *et al.* Two human T cell receptors bind in a similar diagonal mode to the HLA-A2/Tax peptide complex using different TCR amino acids. *Immunity* **8**, 403–411 (1998).
34. Bourcier, K.D. *et al.* Conserved CDR3 regions in T-cell receptor (TCR) CD8$^+$ T cells that recognize the TAX11–19/HLA-A*0201 complex in a subject infected with human T-cell leukemia virus type 1: relationship of T-cell fine specificity and major histocompatibility complex/peptide/tcr crystal structure. *J. Virol.* **75**, 9836–9843 (2001).
35. Garboczi, D.N. *et al.* Structure of the complex between human T-cell receptor, viral peptide and HLA-A2. *Nature* **384**, 134–141 (1996).
36. Garcia, K.C. *et al.* Structural basis of plasticity in T cell receptor recognition of a self peptide-MHC antigen. *Science* **279**, 1166–1172 (1998).
37. Reiser, J.B. *et al.* CDR3 loop flexibility contributes to the degeneracy of TCR recognition. *Nat. Immunol.* **4**, 241–247 (2003).
38. Reiser, J.B. *et al.* Crystal structure of a T cell receptor bound to an allogeneic MHC molecule. *Nat. Immunol.* **1**, 291–297 (2000).
39. Reiser, J.B. *et al.* A T cell receptor CDR3β loop undergoes conformational changes of unprecedented magnitude upon binding to a peptide/MHC class I complex. *Immunity* **16**, 345–354 (2002).
40. Luz, J.G. *et al.* Structural comparison of allogeneic and syngeneic T cell receptor-peptide-major histocompatibility complex complexes: a buried alloreactive mutation subtly alters peptide presentation substantially increasing V_β interactions. *J. Exp. Med.* **195**, 1175–1186 (2002).
41. Baker, B.M., Turner, R.V., Gagnon, S.J., Wiley, D.C. & Biddison, W.E. Identification of a crucial energetic footprint on the α1 helix of human histocompatibility leukocyte antigen (HLA)-A2 that provides functional interactions for recognition by tax peptide/HLA-A2-specific T cell receptors. *J. Exp. Med.* **193**, 551–562 (2001).
42. Baxter, T.K. *et al.* Strategic mutations in the class I major histocompatibility complex HLA-A2 independently affect both peptide binding and T cell receptor recognition. *J. Biol. Chem.* **279**, 29175–29184 (2004).
43. Borg, N.A. *et al.* The CDR3 regions of an immunodominant T cell receptor dictate the 'energetic landscape' of peptide-MHC recognition. *Nat. Immunol.* **6**, 171–180 (2005).
44. Macdonald, W.A. *et al.* A naturally selected dimorphism within the HLA-B44 supertype alters class I structure, peptide repertoire, and T cell recognition. *J. Exp. Med.* **198**, 679–691 (2003).
45. Davies, D.R. & Cohen, G.H. Interactions of protein antigens with antibodies. *Proc. Natl. Acad. Sci. USA* **93**, 7–12 (1996).
46. Tormo, J. *et al.* Crystal structure of a human rhinovirus neutralizing antibody complexed with a peptide derived from viral capsid protein VP2. *EMBO J.* **13**, 2247–2256 (1994).
47. Adams, E.J., Chien, Y.H. & Garcia, K.C. Structure of a $\gamma\delta$ T cell receptor in complex with the nonclassical MHC T22. *Science* **308**, 227–231 (2005).
48. Krogsgaard, M. *et al.* Evidence that structural rearrangements and/or flexibility during TCR binding can contribute to T cell activation. *Mol. Cell* **12**, 1367–1378 (2003).
49. Sim, B.C., Lo, D. & Gascoigne, N.R. Preferential expression of TCR V_α regions in CD4/CD8 subsets: class discrimination or co-receptor recognition? *Immunol. Today* **19**, 276–282 (1998).
50. Krogsgaard, M. *et al.* Agonist/endogenous peptide-MHC heterodimers drive T cell activation and sensitivity. *Nature* **434**, 238–243 (2005).
51. Irvine, D.J., Purbhoo, M.A., Krogsgaard, M. & Davis, M.M. Direct observation of ligand recognition by T cells. *Nature* **419**, 845–849 (2002).
52. Purbhoo, M.A., Irvine, D.J., Huppa, J.B. & Davis, M.M. T cell killing does not require the formation of a stable mature immunological synapse. *Nat. Immunol.* **5**, 524–530 (2004).
53. Jin, L. & Wells, J.A. Dissecting the energetics of an antibody-antigen interface by alanine shaving and molecular grafting. *Protein Sci.* **3**, 2351–2357 (1994).
54. Bass, S.H., Mulkerrin, M.G. & Wells, J.A. A systematic mutational analysis of hormone-binding determinants, in the human growth hormone receptor. *Proc. Natl. Acad. Sci. USA* **88**, 4498–4502 (1991).
55. Claverie, J.M. & Kourilsky, P. The peptidic self model: a reassessment of the role of the major histocompatibility complex molecules in the restriction of the T-cell response. *Ann. Inst. Pasteur Immunol.* **137D**, 425–442 (1986).
56. Macdonald, W. *et al.* Identification of a dominant self-ligand bound to three HLA B44 alleles and the preliminary crystallographic analysis of recombinant forms of each complex. *FEBS Lett.* **527**, 27–32 (2002).
57. Clements, C.S. *et al.* The production, purification and crystallisation of a soluble, heterodimeric form of a highly selected T-cell receptor in its unliganded and liganded state. *Acta Crystallogr. D Biol. Crystallogr. D* **58**, 2131–2134 (2002).
58. Otwinowski, Z. & Minor, W. Processing of X-ray diffraction data collected in oscillation mode. *Methods Enzymol.* **276**, 307–326 (1997).
59. Storoni, L.C., McCoy, A.J. & Read, R.J. Likelihood-enhanced fast rotation functions. *Acta Crystallogr D Biol Crystallogr. D* **60**, 432–438 (2004).
60. Murshudov, G.N., Vagin, A.A. & Dodson, E.J. Refinement of molecular structures by maximum-likelihood method. *Acta Crystallogr D Biol Crystallogr D* **53**, 240–255 (1997).
61. Jones, T.A., Zou, J.Y., Cowan, S.W. & Kjeldgaard. Improved methods for building protein models in electron density maps and the location of errors in these models. *Acta Crystallogr A* **47**, 110–119 (1991).
62. Winn, M.D., Isupov, M.N. & Murshudov, G.N. Use of TLS parameters to model anisotropic displacements in macromolecular refinement. *Acta Crystallogr D Biol Crystallogr D* **57**, 122–133 (2001).
63. Salter, R.D. & Cresswell, P. Impaired assembly and transport of HLA-A and -B antigens in a mutant TxB cell hybrid. *EMBO J.* **5**, 943–949 (1986).
64. Alexander, J., Payne, J.A., Murray, R., Frelinger, J.A. & Cresswell, P. Differential transport requirements of HLA and H-2 class I glycoproteins. *Immunogenetics* **29**, 380–388 (1989).
65. Burrows, S.R. *et al.* T cell receptor repertoire for a viral epitope in humans is diversified by tolerance to a background major histocompatibility complex antigen. *J. Exp. Med.* **182**, 1703–1715 (1995).
66. Lefranc, M.P. IMGT, the international ImMunoGeneTics database. *Nucleic Acids Res.* **29**, 207–209 (2001).